

Article

New Biscembranoids Sardigitolides A–D and Known Cembranoid-Related Compounds from *Sarcophyton digitatum*: Isolation, Structure Elucidation, and Bioactivities

Tzu-Yin Huang ¹, Chiung-Yao Huang ², Chih-Hua Chao ^{3,4} , Chi-Chien Lin ^{5,6} , Chang-Feng Dai ⁷, Jui-Hsin Su ⁸, Ping-Jyun Sung ⁸ , Shih-Hsiung Wu ⁹ and Jyh-Horng Sheu ^{1,2,6,10,*}

- ¹ Doctoral Degree Program in Marine Biotechnology, National Sun Yat-sen University, Kaohsiung 804, Taiwan; slime112229@gmail.com
- ² Department of Marine Biotechnology and Resources, National Sun Yat-sen University, Kaohsiung 804, Taiwan; huangcy@mail.nsysu.edu.tw
- ³ School of Pharmacy, China Medical University, Taichung 404, Taiwan; chchao@mail.cmu.edu.tw
- ⁴ Chinese Medicine Research and Development Center, China Medical University Hospital, Taichung 404, Taiwan
- ⁵ Institute of Biomedical Science, National Chung-Hsing University, Taichung 402, Taiwan; lincc@dragon.nchu.edu.tw
- ⁶ Department of Medical Research, China Medical University Hospital, China Medical University, Taichung 404, Taiwan
- ⁷ Institute of Oceanography, National Taiwan University, Taipei 112, Taiwan; corallab@ntu.edu.tw
- ⁸ National Museum of Marine Biology and Aquarium, Pingtung 944, Taiwan; x2219@nmmba.gov.tw (J.-H.S.); pjsung@nmmba.gov.tw (P.-J.S.)
- ⁹ Institute of Biological Chemistry and Chemical Biology and Molecular Biophysics Program, Taiwan International Graduate Program, Academia Sinica, Taipei 112, Taiwan; shwu@gate.sinica.edu.tw
- ¹⁰ Graduate Institute of Natural Products, Kaohsiung Medical University, Kaohsiung 807, Taiwan
- * Correspondence: sheu@mail.nsysu.edu.tw; Tel.: +886-7-5252000 (ext. 5030); Fax: +886-7-5255020

Received: 7 July 2020; Accepted: 27 August 2020; Published: 29 August 2020



Abstract: Chemical examination from the cultured soft coral *Sarcophyton digitatum* resulted in the isolation and structural identification of four new biscembranoidal metabolites, sardigitolides A–D (1–4), along with three previously isolated biscembranoids, sarcophytolide L (5), glaucumolide A (6), glaucumolide B (7), and two known cembranoids (8 and 9). The chemical structures of all isolates were elucidated on the basis of 1D and 2D NMR spectroscopic analyses. Additionally, in order to discover bioactivity of marine natural products, 1–8 were examined in terms of their inhibitory potential against the upregulation of inflammatory factor production in lipopolysaccharide (LPS)-stimulated murine macrophage J774A.1 cells and their cytotoxicities against a limited panel of cancer cells. The anti-inflammatory results showed that at a concentration of 10 µg/mL, 6 and 8 inhibited the production of IL-1β to 68 ± 1 and 56 ± 1%, respectively, in LPS-stimulated murine macrophages J774A.1. Furthermore, sardigitolide B (2) displayed cytotoxicities toward MCF-7 and MDA-MB-231 cancer cell lines with the IC₅₀ values of 9.6 ± 3.0 and 14.8 ± 4.0 µg/mL, respectively.

Keywords: *Sarcophyton digitatum*; biscembranoid-type metabolites; cytotoxicity; inflammatory factor production; LPS-stimulated murine macrophage

1. Introduction

Cembrane diterpenoids and their derivatives are an abundant and structurally diverse group of secondary metabolites of soft corals and gorgonians. The 14-membered ring structures of cembranoids are biosynthetically formed by cyclization of a geranylgeranyl pyrophosphate precursor between carbons 1 and 14 [1]. These compounds possess a defense mechanism against their natural predators and protect corals against viral infections [2]. Cembranoids exhibit various useful biological properties, such as antitumor [3–8] and anti-inflammatory activities [7,9–12].

Previous studies indicated that species of *Sarcophyton* are rich sources of compounds, such as cembranoids [13–16], biscembranoids [17–21], and steroids [22]. Until now, more than 500 marine natural objects have been found from the soft corals of the genus *Sarcophyton* [23]. It is worth mentioning that biscembranoid-type metabolites are mainly biosynthetically rationalized by a Diels–Alder reaction of two monocembranoidal members, a 1,3-diene cembranoid unit, and a dienophile cembranoid unit. The diene unit forms new trisubstituted conjugated double bonds at C-34/C-35. Normally, most biscembranoids are biosynthesized by the endo-type cyclization of a Diels–Alder reaction [21]. Although many specimens of *Sarcophyton* genus have been chemically studied, there is only one chemical investigation of the soft coral *Sarcophyton digitatum* that has been reported by Zeng et al. in 2000, which led to the isolation of a polyhydroxylated sterol, sardisterol, from this species [24]. Due to the structure diversity and attracting bioactivities of natural products from soft corals, it is well worth further investigating for the discovery of new metabolites from *S. digitatum*. As part of our continuing investigations of discovering bioactive compounds from soft corals, herein is reported the chemical examination of a cultured *S. digitatum*, which resulted in the isolation and structure identification of four new biscembranoidal metabolites, sardigitolides A–D (1–4), along with five known compounds, sarcophytolide L (5) [25], glaucumolide A (6) [18], glaucumolide B (7) [18], isosarcophytonolide D (8) [26], and (4Z,8S,9S,12Z,14E)-9-hydroxy-1-isopropyl-8,12-dimethyloxabicyclo [9.3.2]-hexadeca-4,12,14-trien-18-one (9) [27]. Lipopolysaccharide (LPS), a known endotoxin, is the main component of the outer membrane of gram-negative bacteria, which could induce an inflammatory response in mammalian tissues. In most cases, the inflammatory response helps the organism to clear the LPS or pathogen. However, the violent inflammation caused by overproduced LPS could lead to tissue damage [28]. In the present study, the inhibitory effect of isolates 1–8 against the enhanced production of inflammatory factors in LPS-treated murine macrophage J774A.1 cells was examined. Furthermore, the in vitro cytotoxicities toward MCF-7, MDA-MB-231, HepG2, and HeLa cells of compounds 1–8 were investigated.

2. Results and Discussion

Soft coral *Sarcophyton digitatum* was cultured in the National Museum of Marine Biology & Aquarium. A frozen sample was initially extracted with *n*-hexane and subsequently by ethyl acetate. The ethyl acetate layer was concentrated and repeatedly chromatographed to isolate compounds 1–9 (Figure 1), and structure of new compounds 1–4 were established based on spectroscopic analyses (Supplementary Materials S1–S40).

Sardigitolide A (1) was isolated as a white amorphous powder. High-resolution electron spray ionization mass spectroscopy (HRESIMS) showed a molecular ion peak at m/z 721.4287 $[M + Na]^+$ corresponding to the molecular formula $C_{41}H_{62}O_9$ and implying 11 degrees of unsaturation. In the IR spectrum, a characteristic absorption at 3433 cm^{-1} indicated the presence of a hydroxy group. The ^{13}C spectrum (Table 1) showed 41 carbon signals, including 9 methyl groups, 11 methylene, 10 methines, and 11 quaternary carbons. Its ^1H (Table 2) and ^{13}C NMR spectra revealed signals of three olefinic methyl groups (δ_{H} 1.89, s; 1.86, s; 1.70, s and δ_{C} 26.6; 19.3; 17.9, respectively), two methyl groups linked to oxygen-bearing quaternary carbons (δ_{H} 1.16, s; 1.13, s and δ_{C} 23.7; 25.3, respectively), one methoxy group (δ_{H} 3.55, s; δ_{C} 51.3), an isopropyl group (δ_{H} 2.19, m; 0.95, d, $J = 6.8\text{ Hz}$; 0.76, d, $J = 6.8\text{ Hz}$ and δ_{C} 29.1, CH; 21.1, CH_3 ; 18.3, CH_3 , respectively), two trisubstituted double bond (δ_{H} 6.44, s; δ_{C} 126.0, CH; 160.9, C and δ_{H} 5.06, d, $J = 10.0\text{ Hz}$; 125.2, CH; 138.4, C, respectively), one tetrasubstituted double

bond (δ_C 131.7, C and 130.6, C), three oxygen-bearing methines (δ_H 4.86, t, $J = 6.4$ Hz; 3.49, m; 3.44, dd, $J = 4.0, 12.0$ Hz and δ_C 67.8, CH; 81.7, CH; 73.8, CH, respectively), two oxygen-bearing quaternary carbons (δ_C 73.8, C and 70.4, C), and four carbonyl carbons (δ_C 214.2, C; 210.0, C; 202.5, C; and 174.9, C). All of the above evidence suggested that **1** contained a biscembranoid skeleton. The planar structure of **1** was further determined. The correlations spectroscopy (COSY) signals revealed eight different structural units from H-2 to H₂-36; H₂-6 via H₂-7 and H₂-8; H-9 to H₃-18; isopropyl protons H₃-16 and H₃-17 via H-15, H-12, and H-11; H-21 to H-22; H₂-24 via H₂-25 and H₂-26; H₂-28 via H₂-29 and H-30; and H₂-32 to H-33. These units were assembled by heteronuclear multiple bond correlations (HMBCs) of H₃-16 to C-12, C-15, and C-17; H₃-18 to C-8, C-9, and C-10; H₃-19 to C-4, C-5, and C-6; H₃-37 to C-34, C-35, and C-36; H₃-38 to C-22, C-23, and C-24; H₃-39 to C-27, C-28, and C-29; H₃-40 to C-30, C-31, and C-32; H-2 to C-1, C-3, and C-14; H₂-11 to C-10; H-12 to C-13; H₂-14 to C-1 and C-20; and H-33 to C-34 and C-35. Accordingly, compound **1** had an additional degree of unsaturation, which was suggested to be of an ether ring between C-26 and C-30 established via an HMBC from H-26 to C-30. The gross structure of **1** was thus confirmed as shown in Figure 2 which possesses a biscembranoid skeleton similar to ximaolides E and F [29].

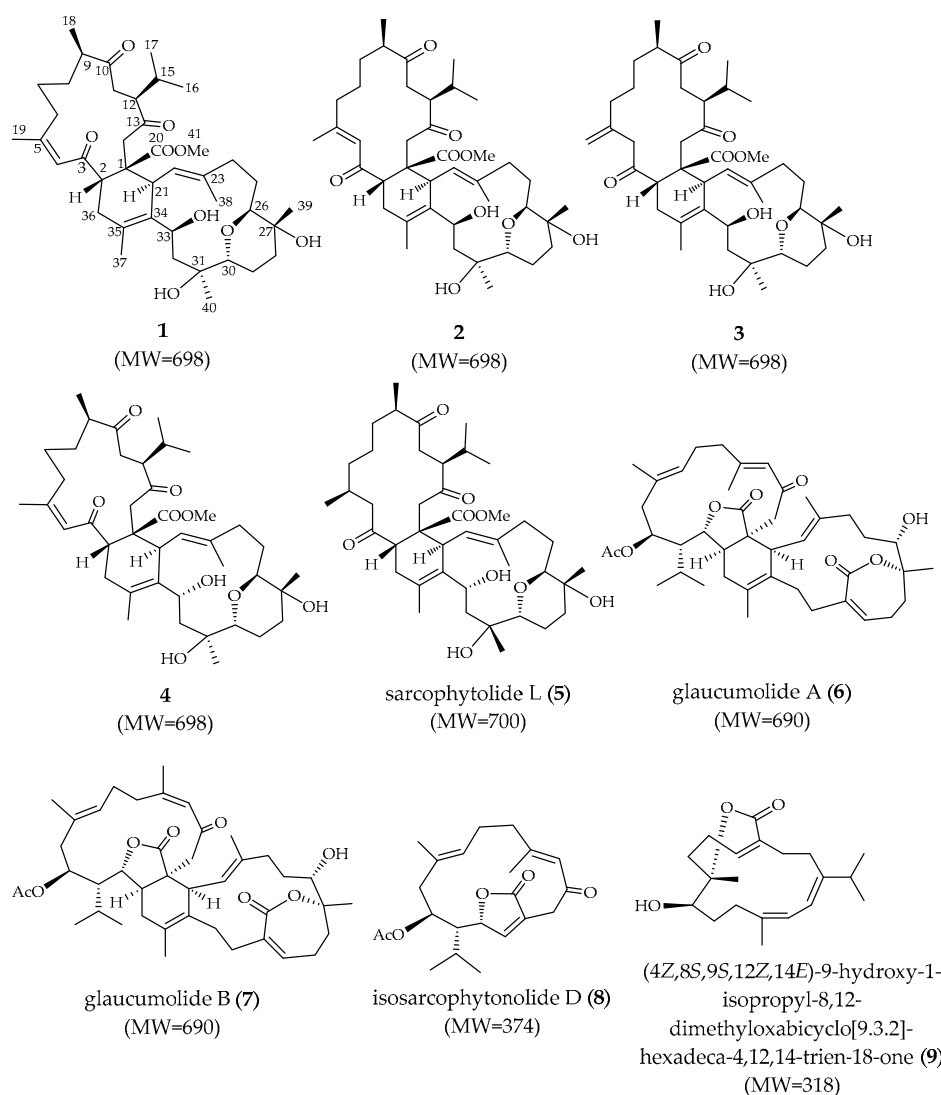


Figure 1. Structures of compounds 1–9.

Table 1. ^{13}C NMR spectroscopic data of 1–4.

Position	1 ^α	2	3	4 ^b
1	50.2 (C)	48.7 (C)	49.8 (C)	49.4 (C)
2	46.0 (CH) ^c	47.3 (CH)	45.8 (CH)	44.0 (CH)
3	202.5 (C)	203.8 (C)	210.3 (C)	201.5 (C)
4	126.0 (CH)	126.0 (CH)	51.0 (CH ₂)	124.7 (CH)
5	160.9 (C)	159.8 (C)	143.2 (C)	159.4 (C)
6	32.3 (CH ₂)	39.8 (CH ₂)	36.5 (CH ₂)	34.0 (CH ₂)
7	24.7 (CH ₂)	24.1 (CH ₂)	25.7 (CH ₂)	25.2 (CH ₂)
8	31.0 (CH ₂)	31.1 (CH ₂)	33.8 (CH ₂)	33.6 (CH ₂)
9	44.6 (CH)	45.7 (CH)	47.7 (CH)	44.7 (CH)
10	214.2 (C)	213.3 (C)	213.6 (C)	213.6 (C)
11	34.7 (CH ₂)	35.1 (CH ₂)	34.2 (CH ₂)	37.1 (CH ₂)
12	52.6 (CH)	52.1 (CH)	51.1 (CH)	52.3 (CH)
13	210.0 (C)	211.2 (C)	211.6 (C)	207.6 (C)
14	46.6 (CH ₂)	47.7 (CH ₂)	46.8 (CH ₂)	45.2 (CH ₂)
15	29.1 (CH)	29.4 (CH)	29.2 (CH)	28.3 (CH)
16	18.3 (CH ₃)	17.9 (CH ₃)	18.4 (CH ₃)	17.3 (CH ₃)
17	21.1 (CH ₃)	20.8 (CH ₃)	21.0 (CH ₃)	21.0 (CH ₃)
18	17.2 (CH ₃)	16.3 (CH ₃)	17.6 (CH ₃)	18.3 (CH ₃)
19	26.6 (CH ₃)	20.3 (CH ₃)	114.9 (CH ₂)	26.4 (CH ₃)
20	174.9 (C)	174.4 (C)	175.0 (C)	174.1 (C)
21	42.9 (CH)	40.8 (CH)	42.5 (CH)	41.7 (CH)
22	125.2 (CH)	124.0 (CH)	124.5 (CH)	126.8 (CH)
23	138.4 (C)	140.2 (C)	139.3 (C)	134.9 (C)
24	36.7 (CH ₂)	38.5 (CH ₂)	37.6 (CH ₂)	34.9 (CH ₂)
25	25.8 (CH ₂)	26.8 (CH ₂)	26.3 (CH ₂)	24.4 (CH ₂)
26	81.7 (CH)	84.8 (CH)	82.7 (CH)	79.8 (CH)
27	70.4 (C)	70.1 (C)	70.4 (C)	69.0 (C)
28	33.6 (CH ₂)	32.0 (CH ₂)	33.2 (CH ₂)	33.6 (CH ₂)
29	19.5 (CH ₂)	19.8 (CH ₂)	19.9 (CH ₂)	19.2 (CH ₂)
30	73.8 (CH)	74.0 (CH)	73.9 (CH)	72.8 (CH)
31	73.8 (C)	74.0 (C)	73.9 (C)	72.8 (C)
32	40.2 (CH ₂)	41.2 (CH ₂)	40.6 (CH ₂)	39.8 (CH ₂)
33	67.8 (CH)	69.9 (CH)	68.5 (CH)	64.9 (CH)
34	131.7 (C)	131.5 (C)	132.8 (C)	132.7 (C)
35	130.6 (C)	130.2 (C)	130.1 (C)	125.2 (C)
36	34.0 (CH ₂)	34.0 (CH ₂)	34.2 (CH ₂)	32.9 (CH ₂)
37	19.3 (CH ₃)	19.8 (CH ₃)	19.6 (CH ₃)	16.8 (CH ₃)
38	17.9 (CH ₃)	18.9 (CH ₃)	18.5 (CH ₃)	17.2 (CH ₃)
39	25.3 (CH ₃)	25.4 (CH ₃)	25.4 (CH ₃)	26.2 (CH ₃)
40	23.7 (CH ₃)	22.9 (CH ₃)	23.4 (CH ₃)	24.7 (CH ₃)
41	51.3 (CH ₃)	51.6 (CH ₃)	51.3 (CH ₃)	50.6 (CH ₃)

^α Spectroscopic data of 1–3 were recorded at 100 MHz in CDCl₃. ^b Spectroscopic data of 4 was recorded at 125 MHz in DMSO-*d*₆. ^c Attached protons were deduced by DEPT experiments.

The relative configuration of **1** was determined by the analysis of correlations recorded by nuclear Overhauser effect spectroscopy (NOESY). As shown in Figure 3, the NOE correlations of H-4 (δ_{H} 6.44, s) with H₃-19 (δ_{H} 1.89, s), together with the obviously downfield-shifted methyl group at C-19 (δ_{C} 26.6, CH₃), suggested a *cis* geometry of C-4/C-5 trisubstituted double bond. Assuming the β -orientations of H₃-41 as previously reported [30], NOE correlations of H₃-41 with both of H₃-16 (δ_{H} 0.76, d, $J = 6.8$ Hz) and H₃-17 (δ_{H} 0.95, d, $J = 6.8$ Hz), and all of H₃-16, H₃-17 and H₃-18 (δ_{H} 1.08, d, $J = 7.2$ Hz) with H-11 (δ_{H} 2.13, m) suggested the β -orientations of H₃-18 and C-1 carbomethoxy groups, on the basis that metabolites of this type with absolute configurations determined previously all possessed 1*S* and 2*S* configurations [30]. Furthermore, the correlations of H-2 with H-22 (δ_{H} 5.06, d, $J = 10.0$ Hz); H-22 with H-24 β (δ_{H} 2.43, m); and H-24 β with H-25 β (δ_{H} 1.84, m); H-25 β with H₃-39 (δ_{H} 1.13, s); H₃-39 with H-28 β (δ_{H} 1.52, m); H-28 β with H-30 (δ_{H} 3.44, dd, $J = 4.0, 12.0$ Hz) reflected the β -orientation of H-30

and H₃-39. In contrast, the α -orientations of H-9 and H-12 were confirmed by the NOE correlations of H-11 α (δ_{H} 2.76, m) with both H-9 (δ_{H} 2.71, m) and H-12 (δ_{H} 2.97, m). The α -orientation of H-26 was determined by the NOE correlations of H-21 (δ_{H} 3.37, m) with H₃-38 (δ_{H} 1.70, s); H₃-38 with H-24 α (δ_{H} 1.98, m); H-24 α with H-25 α (δ_{H} 1.64, m); H-25 α with H-26 (δ_{H} 3.49, m). Also, the α -orientations of H-33 and H₃-40 were determined by the NOE correlations of H-33 (δ_{H} 4.86, t, $J = 6.4$ Hz) with both H₃-37 (δ_{H} 1.86, s) and H₃-40 (δ_{H} 1.16, s). Moreover, the ¹³C NMR signals of C-37 (δ_{C} 19.3, CH₃) and C-38 (δ_{C} 17.9, CH₃) indicated the *E* geometry of the trisubstituted C-22/C-23 and tetrasubstituted C-34/C-35 double bonds. According to the above described evidence, and since compounds of this type are likely biosynthesized from the same or similar precursors and pathway, the absolute configuration of **1** was proposed as 1*S*,2*S*,9*R*,12*S*,21*S*,26*S*,27*R*,30*R*,31*S*,33*S*.

The pseudomolecular ion peak of sardigitolide B (**2**) [M + Na]⁺ at $m/z = 721.4283$ indicated the same molecular formula of **2**, C₄₁H₆₂O₉, as that of **1**. The ¹³C NMR spectrum of **2** showed similar signals to those of **1**. Also, it displayed carbon signals of 9 methyls, 11 methylenes, 10 methines, and 11 quaternary carbons. By detailed analysis of the 2D NMR spectral data of **2**, a similar gross structure to that of **1** was deduced. However, it was found that **2** possesses a remarkably upfield-shifted signal of H-4 (δ_{H} 5.85, s), while **1** displayed a downfield-shifted resonance for H-4 (δ_{H} 6.44, s). Also, the ¹³C NMR spectroscopy data were found to be quite similar to those of **1**, with the exception of CH₃-19 at δ_{C} 26.6 in **1** and δ_{C} 20.3 in **2**, suggesting the presence of a *trans* geometry of 4,5-double bond.

Table 2. ¹H NMR spectroscopic data of **1–4**.

Position	1 ^a	2	3	4 ^b
2	3.59, m	3.73, m	3.74, t (7.6) ^c	3.37, m
4	6.44, s	5.85, s	3.20, m; 3.64 m	6.30, s
6	1.68, m; 3.30, m	1.99, m; 2.21, m	1.80, m; 2.16 m	2.11, m
7	1.34, m; 1.52, m	1.51, m; 1.60, m	1.27, m	1.10, m; 1.30, m
8	1.34, m; 1.64, m	1.49, m	1.52, m; 1.63 m	1.23, m; 1.54, m
9	2.71, m	2.24, m	2.43, m	2.73, m
11	2.13, m; 2.76, m	2.09, m; 2.98, m	2.04, m; 3.0, m	2.05, m; 3.01, m
12	2.97, m	2.82, m	3.05, m	2.99, m
14	2.84, m; 3.11, m	2.58, m; 3.23, m	3.10, m	2.58, m; 2.82, m
15	2.19, m	2.07, m	2.03, m	2.03, m
16	0.76, d (6.8)	0.77, d (6.8)	0.79, d (6.8)	0.59, d (7.0)
17	0.95, d (6.8)	0.94, d (6.8)	0.95, d (6.4)	0.90, d (6.5)
18	1.08, d (7.2)	1.13, d (6.8)	1.13, d (7.2)	0.96, (7.0)
19	1.89, s	2.12, s	4.72, 4.88, brs	1.84, s
21	3.37, m	3.73, d (10.8)	3.50, m	3.36, m
22	5.06, d (10.0)	5.25, d (10.8)	5.17, d (10.4)	4.99, d (10.5)
24	1.98, m; 2.43, m	1.94, m; 2.52, m	1.94, m; 2.50 m	1.82, m; 2.24, m
25	1.64, m; 1.84, m	1.61, m; 1.99, m	1.63, m; 1.94 m	1.58, m; 1.64, m
26	3.49, m	3.60, m	3.54, d (9.6)	3.28, d (10.5)
28	1.52, m; 1.72, m	1.52, m; 1.71, m	1.58, m; 1.72 m	1.62, m; 2.16, m
29	1.57, m; 1.70, m	1.70, m;	1.63, m; 1.71 m	1.29, m; 1.64, m
30	3.44, dd (4.0; 12.0)	3.63, m	3.52, m	3.15, dd (4.0; 12.0)
32	1.55, m; 2.19 m	1.71, m; 1.92, m	1.60, m; 2.03 m	2.19, m
33	4.86, t (6.4)	4.80, t (6.4)	4.83, t (6.4)	4.78, d (10.5)
36	2.26, m	2.26 m; 2.56 m	2.15, m; 2.40, m	1.92, m
37	1.86, s	1.91, s	1.89, s	1.66, s
38	1.70, s	1.77, s	1.75, s	1.57, s
39	1.13, s	1.13, s	1.14, s	0.96, s
40	1.16, s	1.14, s	1.15, s	1.01, s
41	3.55, s	3.58, s	3.58, s	3.40, s

^a Spectroscopic data of **1–3** were recorded at 400 MHz in CDCl₃. ^b Spectroscopic data of **4** was recorded at 500 MHz in DMSO-*d*₆. ^c J values (in Hz) in parentheses.

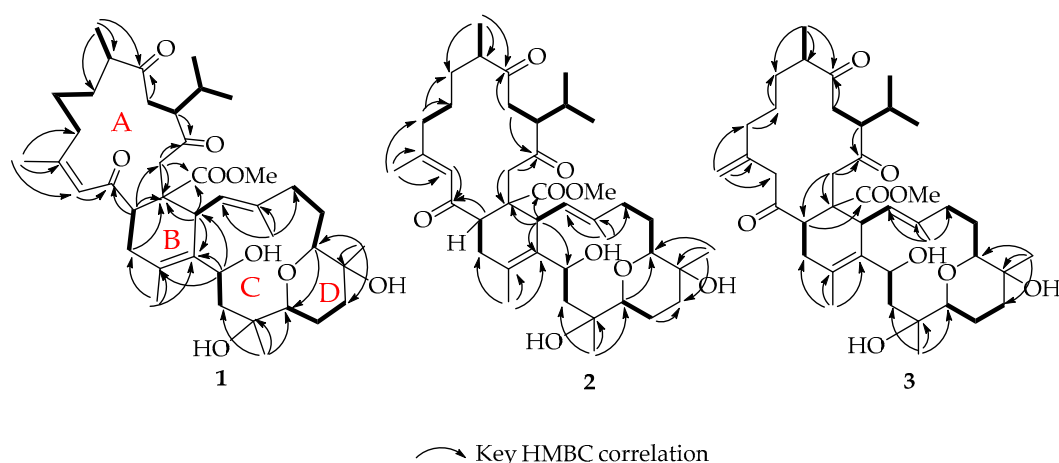


Figure 2. Selected COSY and HMBC correlations of 1–3.

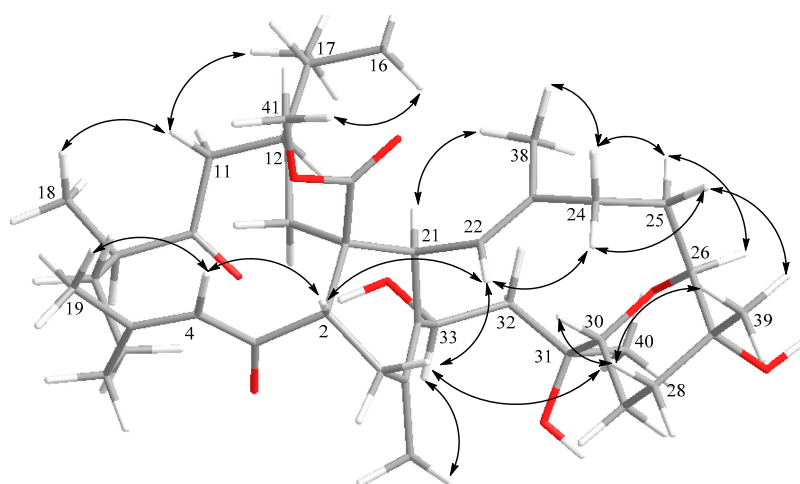


Figure 3. Key NOE correlations of compound 1.

The relative configurations of the stereogenic centers in **2** were determined from the NOESY spectrum, which also showed similar NOE correlations to those of **1**. In contrast, H-4 (δ_{H} 5.85, s) showed an NOE correlation with H-2 (δ_{H} 3.73, m), but not with H₃-19 (δ_{H} 2.12, s), confirming the *E* geometry of the double bond at C-4 and C-5 again. These results determined **2** to be the 4*E* isomer of **1**.

Sardigitolide C (**3**) exhibited a protonated molecular peak at m/z 721.4281 [$M + \text{Na}$]⁺ in the HR-ESI-MS spectrum, establishing the same molecular formula, C₄₁H₆₂O₉, and 11 degrees of unsaturation as those of **1** and **2**. The ¹³C NMR spectroscopy data also showed 41 carbon signals, including 8 methyl groups, 13 methylene, 9 methines, and 11 quaternary carbons. Analyzing the 2D NMR spectral data of **3** in detail showed a similar gross structure of **3** to that of **1**, except that the chemical shifts of CH₂-19 (δ_{H} 4.72, 4.88, brs; δ_{C} 114.9) in **3** indicated the presence of 1,1-disubstituted double bond at C-5/C-19. The relative configuration of **3** was also determined from NOESY spectrum, which showed similar NOE correlations among the corresponding protons to those of **1**. This is the first ximaolide-type compound containing a disubstituted double bond at C-5.

Sardigitolide D (**4**) was isolated as a white amorphous solid. The HR-ESI-MS of **4** showed a pseudomolecular ion peak at 721.4268 [$M + \text{Na}$]⁺, indicating the molecular formula C₄₁H₆₂O₉ and implying 11 degrees of unsaturation. In the ¹³C and DEPT-135 spectra, **4** showed 41 carbon signals resembling those of **1** including 9 methyls, 11 methylenes, 10 methines, and 11 quaternary carbons. Also, **4** had the same gross structure as **1** according to the detailed analyses of 1D and 2D NMR (COSY and HMBC) spectra. However, it was found that H-33 of **4** showed a different coupling constant

($J = 10.5$ Hz) to that of H-33 ($J = 6.4$ Hz) in **1**. Furthermore, **4** did not show NOE correlation between H-22 ($\delta_{\text{H}} 4.99$, d, $J = 10.5$ Hz) and H-33 ($\delta_{\text{H}} 4.78$, d, $J = 10.5$ Hz), while **1–3** exhibited NOE interactions between H-22 and H-33, revealing the 33*R* configuration. On the basis of the above findings, the molecular structure of **4** was determined unambiguously to be the 33-epimer of **1**.

It is known that IL-1 β , the cytokine family member of interleukin-1 produced by activated macrophages, can lead to a strong immune response, and many studies have shown that IL-1 β is related to various diseases, such as rheumatoid arthritis [31,32], neuropathic pain [33], and cardiovascular disease [34]. Furthermore, IL-1 β has been suggested as a therapeutic target for the treatment of diabetic retinopathy [35,36]. In this study, we also attempted to screen the bioactivity of isolates with potential anti-inflammatory and cytotoxic abilities. Therefore, **1–8** were screened for their inhibitory potential against the upregulation of proinflammatory cytokine IL-1 β in LPS-stimulated murine macrophage J774A.1 cells. The results showed that, at a concentration of 10 $\mu\text{g/mL}$, **6** and **8** potentially inhibited LPS-induced IL-1 β production to 68 ± 1 and $56 \pm 1\%$, respectively, with IC_{50} values of 10.7 ± 2.7 and 14.9 ± 5.1 $\mu\text{g/mL}$, respectively. In addition, compounds **1–8** were assayed for their cytotoxicities toward MCF-7, MDA-MB-231, HepG2, and HeLa carcinoma cell lines. The results (Table 3) showed that sardigitolide B (**2**) exhibited inhibitory activity toward MCF-7 and MDA-MB-231 cells with IC_{50} values of 9.6 ± 3.0 and 14.8 ± 4.0 $\mu\text{g/mL}$, respectively, and glaucumolide A (**6**) showed cytotoxicity toward MCF-7, HepG2, and HeLa cell lines with IC_{50} values of 10.1 ± 3.3 , 14.9 ± 3.5 , and 17.1 ± 4.5 $\mu\text{g/mL}$, respectively. Glaucumolide B (**7**) also was found to display cytotoxicity toward MCF-7, MDA-MB-231, and HepG2 cell lines, with IC_{50} values of 9.4 ± 3.0 , 17.8 ± 4.5 , and 14.9 ± 4.2 $\mu\text{g/mL}$, respectively. The monocembranoid **8** (molecular weight 374) showed cytotoxicity against the growth of MCF-7 cancer cell line with IC_{50} value of 10.9 ± 4.3 $\mu\text{g/mL}$ (29.1 ± 11.4 μM). The remaining compounds did not show any effective cytotoxic and anti-inflammatory activities.

Table 3. Cytotoxicities of compounds **1–8**. IC_{50} ($\mu\text{g/mL}$) values are the mean \pm SEM ($n = 3$).

Compound	MCF-7	MDA-MB-231	HepG2	HeLa
1	– ^a	–	–	–
2	9.6 ± 3.0	14.8 ± 4.0	–	–
3	–	–	–	–
4	–	–	–	–
5	–	–	–	–
6	10.1 ± 3.3	–	14.9 ± 3.5	17.1 ± 4.5
7	9.4 ± 3.0	17.8 ± 4.5	14.9 ± 4.2	–
8	10.9 ± 4.3	–	–	–
Doxorubicin	0.7 ± 0.1	1.3 ± 0.2	1.2 ± 0.4	0.4 ± 0.1

^a—> 20 $\mu\text{g/mL}$.

Methyl tortuosoate, also called methyl tetrahydrosarcoate (**10**) (Figure 4), has been frequently discovered to be the dienophile monomeric cembranoid in the Diels–Alder reaction to biosynthesize relevant biscembranoid, while methyl sarcoate (**11**) has been found to be the dienophile part of this series biscembranoids for only one time [37]. Biscembranoids **1** and **4** are the Diels–Alder reaction products using (7*Z*,8)-dehydromethyl tortuosoate (**12**), **2** using (7*E*,8)-dehydromethyl tortuosoate (**13**), and **3** using (7,19)-dehydromethyl tortuosoate (**14**), respectively, as the dienophiles in the biscembranoids biosynthesis. Cembranoids **12–14** are waiting for discovery in future investigations.

Our previous investigation of secondary metabolites from the soft coral *Sarcophyton glaucum* led to the discovery of two biscembranoid-type compounds, glaucumolide A (**6**) and glaucumolide B (**7**) [19]. The absolute configurations of **6**, **7**, and analogs have been confirmed in 2019 by Wen et al. from the X-ray single crystal diffraction of the same compound **6**, isolated from the soft coral *S. trocheliophorum* [20].

Recently, with the development of molecular phylogenetic analysis technology, McFadden et al. suggested that *S. glacum* contained more than seven genetically distinct clades which might be the reason for the continuous discovery of high chemical diversity of secondary metabolites of the soft coral *S. glacum* [38]. For the same reason, it is possible that the corals of *Sarcophyton* genus could generate similar structure bisembranoids as our present study.

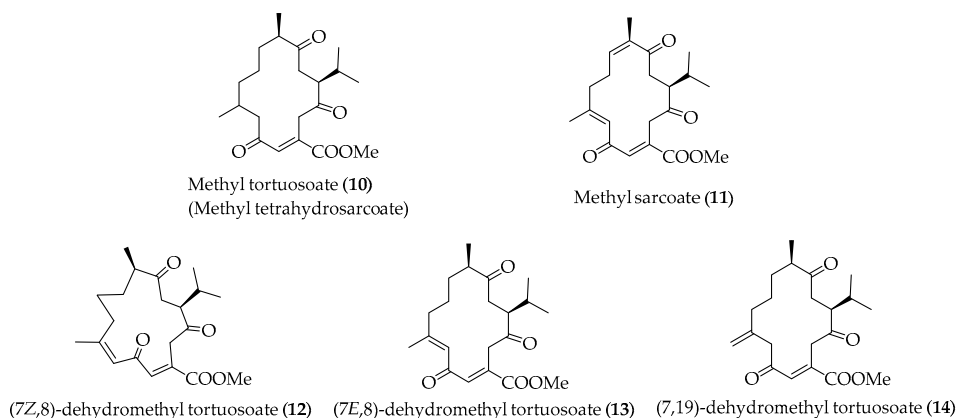


Figure 4. Structures of dienophiles 10–14.

3. Materials and Methods

3.1. General Experimental Procedures

Optical rotations and IR spectra were recorded on a JASCO P-1020 polarimeter and FR/IR-4100 infrared spectrophotometer (Jasco Corporation, Tokyo, Japan), respectively. NMR spectra were acquired on a Varian Unity Inova 500 FT-NMR (Varian Inc., Palo Alto, CA, USA) at 500 and 125 MHz for ^1H and ^{13}C , respectively; or on Varian 400 MR FT-NMR instrument at 400 MHz and 100 MHz for ^1H and ^{13}C , respectively. The data of low-resolution electron spray ionization mass spectroscopy (LRESIMS) were measured by Bruker APEX II mass spectrometer. The data of HRESIMS were obtained by Bruker Apex-Qe 9.4T mass spectrometer. Silica gel 60 and reverse-phased silica gel (RP-18; 230–400 mesh) were used for normal-phase and reverse-phased column chromatography. Precoated silica gel plates (Kieselgel 60 F254, 0.2 mm) (Merck, Darmstadt, Germany) were used for analytical TLC. High-performance liquid chromatography was performed on a Hitachi L-2455 HPLC apparatus with a Supelco C18 column (ODS-3, 5 μm , 250 \times 20 mm; Sciences Inc., Tokyo, Japan).

3.2. Soft Coral Material

The cultured soft coral *Sarcophyton digitatum* of this study was originally collected from the wild in an 80-ton cultivation tank (height 1.6 m) located in the National Museum of Marine Biology and Aquarium, Taiwan. The tank was designed to simulate the fringing reefs in southern Taiwan [39]. The bottom of the tank was covered by a 3–5 cm layer of coral sand, and artificial rocks were distributed on the sand. Sand-filtered seawater pumped directly from the adjacent reef coast and added to the tank at an exchange rate of 10% per day of the total volume. The tank was a semiclosed recirculating aquaculture system and did not require deliberate feeding [40]. The water temperatures were maintained between 24 and 27 $^\circ\text{C}$ via a heat-exchanger cooling system. The soft coral *S. digitatum* was harvested in the National Museum of Marine Biology & Aquarium, Pingtung, in 2014. The coral was identified by one of the authors of this study (C.-F.D.). The animal sample was stored at the Department of Marine Biotechnology and Marine Resources, National Sun Yat-Sen University.

3.3. Extraction and Isolation

A sample of *S. digitatum* (0.9 kg) was sliced and exhaustively extracted with ethyl acetate (1 L × 5), and the solvent-free residue was sequentially partitioned between water and *n*-hexane, ethyl acetate, and *n*-butanol to yield three samples from the above solvents. The resulted EtOAc extract (1.098 g) was purified over silica gel by column chromatography and eluted with acetone in *n*-hexane (10–100%, stepwise), and then with methanol in acetone (0–100%, stepwise) to yield 13 fractions. Fraction 2 was eluted with the solvent system of acetone–*n*-hexane (6:1) to obtain 4 subfractions (A–D). Subfraction 2-B was purified by RP-HPLC using MeOH/H₂O (3:1) at a flow rate of 5 mL/min to afford **8** (2.1 mg). Fraction 3 was eluted with acetone–*n*-hexane (1:5) followed by isolation over a silica gel column to yield 5 subfractions (A–E). Subfraction 3-D was also purified by RP-HPLC with the solvent system of MeOH/H₂O (4:1) at a flow rate of 5 mL/min to obtain **9** (3.4 mg). Fraction 10 was eluted with acetone–*n*-hexane (1:3) and rechromatographed over RP-18 gel to obtain 6 subfractions (A–F). Subfraction 10-F was exhaustively purified by RP-HPLC using MeOH/H₂O (2:1) at a flow rate of 5 mL/min to yield **6** (20.2 mg) and **7** (13.5 mg). Fraction 11, eluting with acetone–*n*-hexane (1:2), was carefully isolated by a reverse-phase silica gel column to yield 6 subfractions (A–F). Subfraction 11-C was further purified by RP-HPLC using MeOH/H₂O (2:1) at a flow rate of 5 mL/min to obtain **1** (8.6 mg), **2** (4.0 mg), **3** (2.5 mg), **4** (2.0 mg), and **5** (23.3 mg).

Compound 1: white powder; $[\alpha]_D^{25} = +48$ (*c* 1.3, CHCl₃), IR (KBr) ν_{\max} 3433, 2958, 1705, 1603, 1436, 1373, 1205, 1135, 1061, 1029 cm⁻¹, ¹³C and ¹H NMR data, Tables 1 and 2; ESIMS *m/z* 721 [M + Na]⁺; HRESIMS *m/z* 721.4287 [M + Na]⁺ (calcd for C₄₁H₆₂O₉Na, 721.4292)

Compound 2: white powder; $[\alpha]_D^{25} = +88$ (*c* 0.1, CHCl₃), IR (KBr) ν_{\max} 3398, 2927, 1704, 1607, 1372, 1204, 1135, 1070 cm⁻¹, ¹³C and ¹H NMR data, Tables 1 and 2; ESIMS *m/z* 721 [M + Na]⁺; HRESIMS *m/z* 721.4283 [M + Na]⁺ (calcd for C₄₁H₆₂O₉Na, 721.4292)

Compound 3: white powder; $[\alpha]_D^{25} = +39$ (*c* 0.8, CHCl₃), IR (KBr) ν_{\max} 3445, 2959, 1703, 1435, 1372, 1206, 1061 cm⁻¹, ¹³C and ¹H NMR data, Tables 1 and 2; ESIMS *m/z* 721 [M + Na]⁺; HRESIMS *m/z* 721.4281 [M + Na]⁺ (calcd for C₄₁H₆₂O₉Na, 721.4292)

Compound 4: white powder; $[\alpha]_D^{25} = +76$ (*c* 0.5, CHCl₃), IR (KBr) ν_{\max} 3446, 2957, 2925, 1706, 1603, 1435, 1375, 1206, 1061 cm⁻¹, ¹³C and ¹H NMR data, Tables 1 and 2; ESIMS *m/z* 721 [M + Na]⁺; HRESIMS *m/z* 721.4268 [M + Na]⁺ (calcd for C₄₁H₆₂O₉Na, 721.4292)

3.4. Cytotoxicity Assay

Cell lines were purchased from the American Type Culture Collection (Rockville, MD). Cytotoxicity assays were carried out using the MTT assays [41]. MCF-7, MDA-MB-231, and HepG2, and HeLa cell lines were cultured and then exposed to various concentrations of **1–8** in dimethyl sulfoxide (DMSO) for 72 h to screen cytotoxicity. Doxorubicin, the positive control of the MTT assay, showed cytotoxicity towards MCF-7, MDA-MB-231, HepG2, and HeLa cancer cell lines, with IC₅₀ values of, 0.7 ± 0.1, 1.3 ± 0.2, 1.2 ± 0.4, and 0.4 ± 0.1 (µg/mL), respectively.

3.5. Anti-Inflammatory Assay

Murine macrophage cell line J774A.1 was purchased from the American Type Culture Collection (Rockville, MD). J774A.1 cells were cultured in 96-well plates at a concentration of 5 × 10⁴ cells/mL and allowed to grow overnight. The cell cultures were added to the DMSO as control or different concentrations of compounds **1–8**, followed by treatment with LPS 1 µg/mL for 24 h. Determination of the cytokine concentration was performed by ELISA according to the manufacturer's protocol and previously reported method [42].

4. Conclusions

Investigation of *Sarcophyton digitatum* led to the purification of four new biscebranoids 1–4, along with five known compounds 5–9. With regards to biological activities, compounds 2, 6, and 7 displayed inhibitory activities against the proliferation of a limited panel of cancer cell lines in a cytotoxic assay. Furthermore, compounds 6 and 8 showed anti-inflammatory activity, which inhibited LPS-induced enhanced IL-1 β production. The soft coral *Sarcophyton* sp. has been shown to produce various biscebranoid metabolites. Up to date, more than 60 biscebranoids biosynthesized via Diels–Alder reaction were isolated. Interestingly, these biscebranoids and their biosynthetic monoscebranoid precursors are often found in *Sarcophyton* species [17–21,30,43–46]. The results of this study suggest that aquaculture of *Sarcophyton* species might produce structurally diversified bioactive compounds that could be beneficial for future drug development. Furthermore, the three dienophiles 12–14 are waiting for discovery as new cebranoids in future studies.

Supplementary Materials: The following are available online at <http://www.mdpi.com/1660-3397/18/9/452/s1>, IR, HRESIMS, ^1H , ^{13}C , distortionless enhancement by polarization transfer (DEPT), heteronuclear single quantum coherence spectroscopy (HSQC), COSY, HMBC, and NOESY spectra of new Compounds 1–4 are available online at <http://www.mdpi.com/1660-3397/18/9/452/s1>, Figure S1: IR spectrum of 1, Figure S2: ESIMS spectrum of 1, Figure S3: HRESIMS spectrum of 1, Figure S4: ^1H NMR spectrum of 1 in CDCl_3 at 400 MHz, Figure S5: ^{13}C NMR spectrum of 1 in CDCl_3 at 100 MHz, Figure S6: DEPT spectrum of 1, Figure S7: HSQC spectrum of 1, Figure S8: COSY spectrum of 1, Figure S9: HMBC spectrum of 1, Figure S10: NOESY spectrum of 1, Figure S11: IR spectrum of 2, Figure S12: ESIMS spectrum of 2, Figure S13: HRESIMS spectrum of 2, Figure S14: ^1H NMR spectrum of 2 in CDCl_3 at 400 MHz, Figure S15: ^{13}C NMR spectrum of 2 in CDCl_3 at 100 MHz, Figure S16: DEPT spectrum of 2, Figure S17: HSQC spectrum of 2, Figure S18: COSY spectrum of 2, Figure S19: HMBC spectrum of 2, Figure S20: NOESY spectrum of 2, Figure S21: IR spectrum of 3, Figure S22: ESIMS spectrum of 3, Figure S23: HRESIMS spectrum of 3, Figure S24: ^1H NMR spectrum of 3 in CDCl_3 at 400 MHz, Figure S25: ^{13}C NMR spectrum of 3 in CDCl_3 at 100 MHz, Figure S26: DEPT spectrum of 2, Figure S27: HSQC spectrum of 3, Figure S28: COSY spectrum of 3, Figure S29: HMBC spectrum of 3, Figure S30: NOESY spectrum of 3, Figure S31: IR spectrum of 4, Figure S32: ESIMS spectrum of 3, Figure S33: HRESIMS spectrum of 4, Figure S34: ^1H NMR spectrum of 4 in $\text{DMSO}-d_6$ at 500 MHz, Figure S35: ^{13}C NMR spectrum of 4 in $\text{DMSO}-d_6$ at 125 MHz, Figure S36: DEPT spectrum of 4, Figure S37: HSQC spectrum of 4, Figure S38: COSY spectrum of 4, Figure S39: HMBC spectrum of 4, Figure S40: NOESY spectrum of 4, Figure S41: ESIMS spectrum of 5, Figure S42: ^1H NMR spectrum of 5 in CDCl_3 at 400 MHz, Figure S43: ^{13}C NMR spectrum of 5 in CDCl_3 at 100 MHz, Figure S44: ESIMS spectrum of 6, Figure S45: ^1H NMR spectrum of 6 in CDCl_3 at 400 MHz, Figure S46: ^{13}C NMR spectrum of 6 in CDCl_3 at 100 MHz, Figure S47: ESIMS spectrum of 7, Figure S48: ^1H NMR spectrum of 7 in CDCl_3 at 400 MHz, Figure S49: ^{13}C NMR spectrum of 7 in CDCl_3 at 100 MHz, Figure S50: ESIMS spectrum of 8, Figure S51: ^1H NMR spectrum of 8 in CDCl_3 at 500 MHz, Figure S52: ^{13}C NMR spectrum of 8 in CDCl_3 at 125 MHz.

Author Contributions: Conceptualization, J.-H.S. (Jyh-Horng Sheu); investigation, T.-Y.H., C.-Y.H., C.-C.L., C.-F.D., J.-H.S. (Jui-Hsin Su), P.-J.S., and J.-H.S. (Jyh-Horng Sheu); writing-original draft, T.-Y.H., C.-Y.H., C.-H.C., and S.-H.W.; writing-review and editing, T.-Y.H., C.-H.C., S.-H.W., and J.-H.S. (Jyh-Horng Sheu); material resources, C.-C.L., C.-F.D., J.-H.S. (Jui-Hsin Su), and P.-J.S. All authors have read and agreed to the published version of the manuscript.

Funding: This research was mainly funded by the Ministry of Science and Technology of Taiwan (MOST 104-2113-M-110-006, 104-2320-B-110-001-MY2, and 107-2320-B-110-001-MY3).

Acknowledgments: Financial support of this work from the Ministry of Science and Technology of Taiwan (MOST 104-2113-M-110-006, 104-2320-B-110-001-MY2, and 107-2320-B-110-001-MY3) to J.-H.S. is gratefully acknowledged.

Conflicts of Interest: The authors declare no conflict of interest.

References

1. Rodríguez, A.D.; Li, Y.; Dhasmana, H. New marine cebranone diterpenoids isolated from the Caribbean gorgonian *Eunicea mammosa*. *J. Nat. Prod.* **1993**, *7*, 1101–1113. [[CrossRef](#)]
2. Katsuyama, I.; Fahmy, H.; Zjawiony, J.K.; Khalifa, S.I.; Kilada, R.W.; Konoshima, T.; Takasaki, M.; Tokuda, H. Semisynthesis of new sarcophine derivatives with chemopreventive activity. *J. Nat. Prod.* **2002**, *65*, 1809–1814. [[CrossRef](#)]

3. Hegazy, M.E.F.; Elshamy, A.I.; Mohamed, T.A.; Hamed, A.R.; Ibrahim, M.A.A.; Ohta, S.; Paré, P.W. Cembrene diterpenoids with ether linkages from *Sarcophyton ehrenbergi*: An anti-proliferation and molecular-docking assessment. *Mar. Drugs* **2017**, *15*, 192. [[CrossRef](#)]
4. Tang, G.H.; Sun, Z.H.; Zou, Y.H.; Yin, S. New cembrane-type diterpenoids from the South China Sea soft coral *Sarcophyton ehrenbergi*. *Molecules* **2016**, *21*, 587. [[CrossRef](#)]
5. Hegazy, M.E.F.; Mohamed, T.A.; Elshamy, A.I.; Hamed, A.R.; Ibrahim, M.A.A.; Ohta, S.; Umeyama, A.; Paré, P.W.; Efferth, T. Sarcophytenolides D–F: Cytotoxic cembrene diterpenoids from the soft coral *Sarcophyton ehrenbergi*. *RSC Adv.* **2019**, *9*, 27183–27189. [[CrossRef](#)]
6. Hassan, H.M.; Rateb, M.E.; Hassan, M.H.; Sayed, A.M.; Shabana, S.; Raslan, M.; Amin, E.; Behery, F.A.; Ahmed, O.M.; Bin Muhsinah, A.; et al. New antiproliferative cembrane diterpenes from the Red Sea *Sarcophyton* species. *Mar. Drugs* **2019**, *17*, 411. [[CrossRef](#)] [[PubMed](#)]
7. Li, S.W.; Ye, F.; Zhu, Z.D.; Huang, H.; Mao, S.C.; Guo, Y.W. Cembrane-type diterpenoids from the South China Sea soft coral *Sarcophyton mililatensis*. *Acta Pharm. Sin. B* **2018**, *8*, 944–955. [[CrossRef](#)] [[PubMed](#)]
8. Sala, G.D.; Agriesti, F.; Mazzoccoli, C.; Tataranni, T.; Costantino, V.; Piccoli, C. Clogging the ubiquitin-proteasome machinery with marine natural products: Last decade update. *Mar. Drugs* **2018**, *16*, 467. [[CrossRef](#)] [[PubMed](#)]
9. Li, G.; Li, H.; Zhang, Q.; Yang, M.; Gu, Y.C.; Liang, L.F.; Tang, W.; Guo, Y.W. Rare cembranoids from Chinese soft coral *Sarcophyton ehrenbergi*: Structural and stereochemical studies. *J. Org. Chem.* **2019**, *84*, 5091–5098. [[CrossRef](#)] [[PubMed](#)]
10. Peng, C.C.; Huang, C.Y.; Ahmed, A.F.; Hwang, T.L.; Dai, C.F.; Sheu, J.H. New cembranoids and a biscembranoid peroxide from the soft coral *Sarcophyton cherbonnieri*. *Mar. Drugs* **2018**, *16*, 276. [[CrossRef](#)]
11. Ahmed, A.F.; Chen, Y.W.; Huang, C.Y.; Tseng, Y.J.; Lin, C.C.; Dai, C.F.; Wu, Y.C.; Sheu, J.H. Isolation and structure elucidation of cembranoids from a Dongsha Atoll soft coral *Sarcophyton stellatum*. *Mar. Drugs* **2018**, *16*, 210. [[CrossRef](#)]
12. Kamada, T.; Kang, M.C.; Phan, C.S.; Zamil, I.I.; Jeon, Y.J.; Vairappan, C.S. Bioactive cembranoids from the soft coral genus *Sinularia* sp. in Borneo. *Mar. Drugs* **2018**, *16*, 99. [[CrossRef](#)] [[PubMed](#)]
13. Lin, W.Y.; Chen, B.W.; Huang, C.Y.; Wen, Z.H.; Sung, P.J.; Su, J.H.; Dai, C.F.; Sheu, J.H. Bioactive cembranoids, sarcocrassocolides P–R, from the Dongsha Atoll soft coral *Sarcophyton crassocaule*. *Mar. Drugs* **2014**, *12*, 840–850. [[CrossRef](#)] [[PubMed](#)]
14. Lin, W.Y.; Su, J.H.; Wen, Z.H.; Kuo, Y.H.; Sheu, J.H. Cytotoxic and anti-inflammatory cembranoids from the Dongsha Atoll soft coral *Sarcophyton crassocaule*. *Bioorganic Med. Chem.* **2010**, *18*, 1936–1941. [[CrossRef](#)] [[PubMed](#)]
15. Huang, H.C.; Ahmed, A.F.; Su, J.H.; Chao, C.H.; Wu, Y.C.; Chiang, M.Y.; Sheu, J.H. Crassocolides A–F, Cembranoids with a *trans*-Fused Lactone from the Soft Coral *Sarcophyton crassocaule*. *J. Nat. Prod.* **2006**, *69*, 1554–1559. [[CrossRef](#)] [[PubMed](#)]
16. Chao, C.H.; Li, W.L.; Huang, C.Y.; Ahmed, A.F.; Dai, C.F.; Wu, Y.C.; Lu, M.C.; Liaw, C.C.; Sheu, J.H. Isoprenoids from the soft coral *Sarcophyton glaucum*. *Mar. Drugs* **2017**, *15*, 202. [[CrossRef](#)]
17. Jia, R.; Kurtán, T.; Mándi, A.; Yan, X.H.; Zhang, W.; Guo, Y.W. Biscembranoids formed from an α,β -unsaturated γ -lactone ring as a dienophile: Structure revision and establishment of their absolute configurations using theoretical calculations of electronic circular dichroism spectra. *J. Org. Chem.* **2013**, *78*, 3113–3119. [[CrossRef](#)] [[PubMed](#)]
18. Huang, C.Y.; Sung, P.J.; Uvarani, C.; Su, J.H.; Lu, M.C.; Hwang, T.L.; Dai, C.F.; Sheu, J.H. Glaucumolides A and B, biscembranoids with new structural type from a cultured soft coral *Sarcophyton glaucum*. *Sci. Rep.* **2015**, *5*, 15624. [[CrossRef](#)] [[PubMed](#)]
19. Sun, P.; Yu, Q.; Li, J.; Riccio, R.; Lauro, G.; Bifulco, G.; Kurtán, T.; Mándi, A.; Tang, H.; Li, T.J.; et al. Bissubvilides A and B, cembrane–capnosane heterodimers from the soft coral *Sarcophyton subviride*. *J. Nat. Prod.* **2016**, *79*, 2552–2558. [[CrossRef](#)]
20. Sun, P.; Cai, F.Y.; Lauro, G.; Tang, H.; Su, L.; Wang, H.L.; Li, H.H.; Mándi, A.; Kurtán, T.; Riccio, R.; et al. Immunomodulatory biscembranoids and assignment of their relative and absolute configurations: Data set modulation in the density functional theory/nuclear magnetic resonance approach. *J. Nat. Prod.* **2019**, *82*, 1264–1273. [[CrossRef](#)]
21. Yan, P.C.; Lv, Y.; van Ofwegen, L.; Proksch, P.; Lin, W.H. Lobophytone A–G, new isobiscembranoids from the soft coral *Lobophytum pauciflorum*. *Org. Lett.* **2010**, *12*, 2484–2487. [[CrossRef](#)] [[PubMed](#)]

22. Zubair, M.S.; Al-Footy, K.O.; Ayyed, S.-E.N.; Al-Lihaibi, S.S.; Alarif, W.M. A review of steroids from *Sarcophyton* species. *Nat. Prod. Res.* **2016**, *30*, 869–879. [[CrossRef](#)] [[PubMed](#)]
23. Elkhawas, Y.A.; Elissawy, A.M.; Elnaggar, M.S.; Mostafa, N.M.; Al-Sayed, E.; Bishr, M.M.; Singab, A.N.B.; Salama, O.M. Chemical diversity in species belonging to soft coral genus *Sarcophyton* and its impact on biological activity: A review. *Mar. Drugs* **2020**, *18*, 41. [[CrossRef](#)] [[PubMed](#)]
24. Su, J.Y.; Yang, R.L.; Zeng, L.M. Sardisterol, a new polyhydroxylated sterol from the soft coral *Sarcophyton digitatum* moser. *Chin. J. Chem.* **2001**, *19*, 515–517. [[CrossRef](#)]
25. Xi, Z.F.; Bie, W.; Chen, W.; Liu, D.; van Ofwegen, L.; Proksch, P.; Lin, W.H. Sarcophytolides G–L, new biscembranoids from the soft coral *Sarcophyton elegans*. *Helv. Chim. Acta.* **2013**, *96*, 2218–2227. [[CrossRef](#)]
26. Yan, X.H.; Gavagnin, M.; Cimino, G.; Guo, Y.W. Two new biscembranes with unprecedented carbon skeleton and their probable biogenetic precursor from the Hainan soft coral *Sarcophyton latum*. *Tetrahedron Lett.* **2007**, *48*, 5313–5316. [[CrossRef](#)]
27. Gross, H.; Wright, A.D.; Beli, W.; König, G.M. Two new bicyclic cembranolides from a new *Sarcophyton* species and determination of the absolute configuration of sarcoglaucol-16-one. *Org. Biomol. Chem.* **2004**, *2*, 1133–1138. [[CrossRef](#)] [[PubMed](#)]
28. Fang, H.; Liu, A.; Chen, X.; Cheng, W.; Dirsch, O.; Dahmen, U. The severity of LPS induced inflammatory injury is negatively associated with the functional liver mass after LPS injection in rat model. *J. Inflamm.* **2018**, *15*, 21. [[CrossRef](#)]
29. Jia, R.; Guo, Y.W.; Chen, P.; Yang, Y.M.; Mollo, E.; Gavagnin, M.; Cimino, G. Biscembranoids and their probable biogenetic precursor from the Hainan soft coral *Sarcophyton tortuosum*. *J. Nat. Prod.* **2007**, *70*, 1158–1166. [[CrossRef](#)]
30. Kurtán, T.; Jia, R.; Li, Y.; Pescitelli, G.; Guo, Y.W. Absolute configuration of highly flexible natural products by the solid-state ECD/TDDFT method: Ximaolides and sinularparvalides. *Eur. J. Org. Chem.* **2012**, *34*, 6722–6728. [[CrossRef](#)]
31. Dayer, J.M.; Oliviero, F.; Punzi, L. A brief history of IL-1 and IL-1 Ra in rheumatology. *Front. Pharmacol.* **2017**, *8*, 293. [[CrossRef](#)] [[PubMed](#)]
32. Kay, J.; Calabrese, L. The role of interleukin-1 in the pathogenesis of rheumatoid arthritis. *Rheumatology* **2004**, *43*, iii2–iii9. [[CrossRef](#)] [[PubMed](#)]
33. Gui, W.S.; Wei, X.; Mai, C.L.; Murugan, M.; Wu, L.J.; Xin, W.J.; Zhou, L.J.; Liu, X.G. Interleukin-1 β overproduction is a common cause for neuropathic pain, memory deficit, and depression following peripheral nerve injury in rodents. *Mol. Pain* **2016**, *12*, 1–15. [[CrossRef](#)] [[PubMed](#)]
34. Szekely, Y.; Arbel, Y. A review of interleukin-1 in heart disease: Where do we stand today? *Cardiol. Ther.* **2018**, *7*, 25–44. [[CrossRef](#)] [[PubMed](#)]
35. Liu, Y.; Costa, M.B.; Gerhardinger, C. IL-1 β is upregulated in the diabetic retina and retinal vessels: Cell-specific effect of high glucose and IL-1 β autostimulation. *PLoS ONE* **2012**, *7*, e36949. [[CrossRef](#)]
36. Kowluru, R.A.; Odenbach, S. Role of interleukin-1 β in the pathogenesis of diabetic retinopathy. *Br. J. Ophthalmol.* **2004**, *88*, 1343–1347. [[CrossRef](#)]
37. Ichige, T.; Okano, Y.; Kanoh, N.; Nakata, M. Total synthesis of methyl sarcophytoate, a marine natural biscembranoid. *J. Org. Chem.* **2009**, *74*, 230–243. [[CrossRef](#)]
38. Maloney, K.N.; Botts, R.T.; Davis, T.S.; Okada, B.K.; Maloney, E.M.; Leber, C.A.; Alvarado, O.; Brayton, C.; Caraballo-Rodríguez, A.M.; Chari, J.V.; et al. Cryptic species account for the seemingly idiosyncratic secondary metabolism of *Sarcophyton glaucum* specimens collected in Palau. *J. Nat. Prod.* **2020**, *83*, 693–705. [[CrossRef](#)]
39. Liu, P.J.; Lin, S.M.; Fan, T.Y.; Meng, P.J.; Shao, K.T.; Lin, H.J. Rates of overgrowth by macroalgae and attack by sea anemones are greater for live coral than dead coral under conditions of nutrient enrichment. *Limnol. Oceanogr.* **2009**, *54*, 1167–1175. [[CrossRef](#)]
40. Chou, W.C.; Liu, P.J.; Chen, Y.H.; Huang, W.J. Contrasting changes in diel variation of net community calcification support that carbonate dissolution can be more sensitive to ocean acidification than coral calcification. *Front. Mar. Sci.* **2020**, *7*, 3. [[CrossRef](#)]
41. Cole, S.P.C. Rapid chemosensitivity testing of human lung tumor cells using the MTT assay. *Cancer Chemother. Pharmacol.* **1986**, *17*, 259–263. [[CrossRef](#)] [[PubMed](#)]

42. Chen, L.; Lin, S.X.; Agha-Majzoub, R.; Overbergh, L.; Mathieu, C.; Chan, L.S. CCL27 is a critical factor for the development of atopic dermatitis in the keratin-14 IL-4 transgenic mouse model. *Int. Immunol.* **2006**, *18*, 1233–1242. [[CrossRef](#)] [[PubMed](#)]
43. Feller, M.; Rudi, A.; Berer, N.; Goldberg, I.; Stein, Z.; Benayahu, Y.; Schleyer, M.; Kashman, Y. Isoprenoids of the soft coral *Sarcophyton glaucum*: nyalolide, a new biscembranoid, and other terpenoids. *J. Nat. Prod.* **2004**, *67*, 1303–1308. [[CrossRef](#)] [[PubMed](#)]
44. Zeng, L.M.; Lan, W.J.; Su, J.Y.; Zhang, G.W.; Feng, X.L.; Liang, Y.J.; Yang, X.P. Two new cytotoxic tetracyclic tetraterpenoids from the Soft coral *Sarcophyton tortuosum*. *J. Nat. Prod.* **2004**, *67*, 1915–1918. [[CrossRef](#)] [[PubMed](#)]
45. Yan, P.C.; Deng, Z.W.; van Ofwegen, L.; Proksch, P.; Lin, W.H. Lobophytone O–T, new biscembranoids and cembranoid from soft coral *Lobophytum pauciflorum*. *Mar. Drugs* **2010**, *8*, 2837–2848. [[CrossRef](#)] [[PubMed](#)]
46. Yan, P.C.; Deng, Z.W.; van Ofwegen, L.; Proksch, P.; Lin, W.H. Lobophytone U–Z₁, biscembranoids from the chinese soft coral *Lobophytum pauciflorum*. *Chem. Biodivers.* **2011**, *8*, 1724–1734. [[CrossRef](#)] [[PubMed](#)]



© 2020 by the authors. Licensee MDPI, Basel, Switzerland. This article is an open access article distributed under the terms and conditions of the Creative Commons Attribution (CC BY) license (<http://creativecommons.org/licenses/by/4.0/>).